PHARMACOPHORE BASED 3D QSAR STUDIES OF SOME BIPHENYLS DERIVATIVES AS PROTEIN TYROSINE PHOSPHATES 1B INHIBITORS

Dwivedi Sunil Kumar[1]*, Paliwal Sarvesh Kumar[2]

Abstract:-
Protein tyrosine phosphates (PTPs) are enzymes that catalyze protein tyrosine dephosphorylation. Among various members of the PTP super family, Protein tyrosine phosphates 1B (PTP1B) has emerged as the best-validated drug target. Mounting evidence from biochemical, genetic and pharmacological studies support a role for PTP1B as a negative regulator in both insulin and leptin signaling collectively. A computer assisted methodology was applied for the construction of pharmacophore and for building 3D QSAR model of novel benzofuran and benzothiophene biphenyl derivatives as a inhibitors of PTP1B. 3D QSAR model of PTB 1B inhibitor based on common featured pharmacophore was developed using phase module of Schrodinger software. In this study A series of 136 analogues of novel benzofuran and benzothiophene biphenyl derivatives as a inhibitors of Protein Tyrosine Phosphatase 1B and their PTP1B inhibitory data (IC_{50}) was selected and used to develop the Pharmacophore based 3D QSAR model. The statistically best model corresponding to PLS 5 (ARRRR.389_5) was selected on the basis of highest values of R^2, 0.9527; SD, 0.1276; and F-value, 297.8. The best model was validated for its stability (Q^2) and reliability to predict the biological activity of the molecules that have not been used for the development of model i.e. test set molecules (Pearson-r). The model showed good values of Q^2 and pearson-r i.e. 0.3655 and 0.611 respectively. The correlation graph between experimental and predicted activities of test and training set molecules was analyze and generated QSAR models should satisfy $q^2 > 0.5$, $R^2 > 0.6$, R^2_o or R'^2_o close to R^2, and the corresponding $0.85 \leq k \leq 1.15$ or $0.85 \leq k' \leq 1.15$. The best model showed satisfactory values of k, 0.998; k', 1.001; R^2_o, 0.999 and R'^2_o, 0.999. These all parameters further strengthen the stability and reliability of generated QSAR model.

Keywords:- Pharmacophore Based 3D QSAR, Protein Tyrosine Phosphatase 1B inhibitor, Schrodinger, PHASE, Diabetes

[1*,2] Department of Pharmacy, Banasthali Vidyapith, Rajasthan INDIA[2].

***Corresponding Author**: Sunil Kumar Dwivedi
[*]Department of Pharmacy, Banasthali Vidyapith, Rajasthan INDIA, Email: sunild2d@gmail.com

DOI: 10.48047/ecb/2023.12.si5a.0257

INTRODUCTION

Protein tyrosine phosphates (PTPs) are enzymes that catalyze protein tyrosine dephosphorylation. In humans, more than a hundred PTPs exist that can function either as negative or positive modulators in various signal transduction pathways[1]. Deregulation of PTP activity contributes to the pathogenesis of several human diseases, including cancer, diabetes and immune disorders [2-4].

The importance of the PTPs in diverse pathophysiology has made them the focus of intense interest as a new class of drug targets. Thus, inhibitors of the PTPs are also expected to have therapeutic value with novel modes of action [5-6]. Among various members of the PTP super family, Protein tyrosine phosphates 1B (PTP1B) has emerged as the best-validated drug target[7]. PTP1B is localized in the cytoplasmic face of the endoplasmic reticulum and is expressed ubiquitously in the classical insulin-targeted tissues such as liver, muscle and fat[8]. Mounting evidence from biochemical, genetic and pharmacological studies support a role for PTP1B as a negative regulator in both insulin and leptin signaling.

PTP1B can associate with dephosphorylated activated insulin receptor (IR) or insulin receptor substrates (IRS)[9-14]. Over expression of PTP1B in cell cultures decreases insulin-stimulated phosphorylation of IR and/ or IRS-1, whereas reduction in the level of PTP1B, by antisense oligonucleotides or neutralizing antibodies, augments insulin initiated signaling [15-18].

Mice that lack PTP1B display enhanced sensitivity to insulin, with increased or prolonged tyrosine phosphorylation of IR in muscle and liver[19-21]. Interestingly, PTP1B *ob/ob* mice are protected against weight gain and have significantly lower triglyceride levels when placed on a high-fat diet. This is unexpected because insulin is also an anabolic factor, and increased insulin sensitivity can result in increased weight gain. PTP1B was subsequently shown to bind and dephosphorylate Janus Kinase2 (JAK2), which is downstream of leptin receptor[22].

Thus, the resistance to diet-induced obesity observed in PTP1B *ob/ob* mice is likely to be associated with increased energy expenditure owing to enhanced leptin sensitivity. Collectively, this biochemical, genetic and pharmacological studies provide strong proof and validating to the concept that inhibition of PTP1B could address both diabetes and obesity and making PTP1B an exciting target for drug development. Selectivity is one of the major issues in the development of PTP1B inhibitors as drugs. Because all PTPs share a high degree of structural conservation in the active site, the pTyr (phosphotyrosine)-binding pocket, designing inhibitors with both high affinity and selectivity for PTP1B poses a challenge. Fortunately, PTP substrate specificity studies have shown that pTyr alone is not sufficient for high-affinity binding, and residues flanking the pTyr are important for PTP substrate recognition[23]. The various research results indicate that there are sub pockets adjacent to the PTP active site that can also be targeted for inhibitor development.

These studies also provide a molecular basis for addressing and manipulating PTP inhibitor potency and specificity, and suggest a novel paradigm for the design of potent and specific PTP inhibitors, namely bidentate ligands that bind to both the active site and a unique adjacent peripheral site. Bioavailability is another important issue in the development of PTP1B-based small-molecule therapeutics.

The active sites of PTPs have evolved to accommodate pTyr, which contains two negative charges at physiological pH. Consequently, most active-site-directed PTP inhibitors (non-hydrolyzable pTyr mimetics) reported to date possess a high charge density to serve as competitive inhibitors[24-25]. A computer assisted methodology was applied for the construction of pharmacophore and for building 3D QSAR model of novel benzofuran and benzothiophene biphenyl derivatives as a inhibitors of PTP1B .

The application of the resulting pharmacophore model in screening database allowed us to identify a small set of other compounds that must be having PTP 1B inhibitor activity. 3D QSAR model of PTB 1B inhibitor based on common featured pharmacophore was developed using phase module of Schrodinger software.

Phase is a software package designed for pharmacophore modelling, structure alignment and activity prediction. Notably this package provides the means to align sets of ligands onto a pharmacophore and to develop 3D-QSAR models able to identify further structural features that govern activity of molecules[26]. In this study Phase was initially applied to develop a common feature PTP 1B inhibitor pharmacophore model to be used

as an alignment rule and, then, to carry out a 3D-QSAR investigation.

MATERIALS AND METHODS

Selection of molecules and data set

A series of 136 analogues of novel benzofuran and benzothiophene biphenyl derivatives as a inhibitors of Protein Tyrosine Phosphatase 1B and their PTP1B inhibitory data (IC_{50}) was selected from published literature[27] and used to develop the Pharmacophore based 3D QSAR model. Out of the total 136 analogues, 22 analogues were removed from the series i.e. analogue SKD-53, SKD-54, SKD-55, SKD-59, SKD-64, SKD-65, SKD-69, SKD-70, SKD-93, SKD-94, SKD-101, SKD-102, SKD-135, SKD-144, SKD-150, SKD-161, SKD-173 was removed because of negative IC_{50} values; analogue SKD-66 SKD-68, SKD-95, SKD-141 and SKD-142 was removed because of unpublished stereochemistry. A total data set of 113 analogues of Benzofuran and Benzothiophene Biphenyls derivative was selected. The biological activities (IC_{50}) were converted into the corresponding pIC_{50} values (-log IC_{50}), where IC_{50} value represents the amount of drug in molar (M) concentration that causes 50% inhibition of Protein Tyrosine Phosphatase 1B. IC_{50} values of all molecules present in dataset were obtained using a same assay method i.e SAS release 6.08, PROCNLIN in malachite green ammonium molybdate method[28].

The pIC_{50} values of the study molecules span over a wide range of activity i.e 5.51 to 7.57. For the development of 3D QSAR model the data set was divided into training set and test set of 80 and 33 molecules respectively. The structures of the study molecules and their corresponding biological activities (IC_{50}) are given in Table I.

Table 1. Chemical structures of dataset used for pharmacophore and 3D QSAR analysis With actual and predicted activities from the best model**.**

SN.	Ligand Name	IC_{50} (µM)	Activity (pIC_{50})		Pharm Set	QSAR Set
1	SKD -52	0.74	6.131	6.04	-	Training
2	SKD -56	0.92	6.036	6.2	-	Training
3	SKD -57	0.74	6.131	5.98	-	Training
4	SKD -58	0.7	6.155	6.01	-	Training
5	SKD -60	1.08	5.967	6.04	-	Training
6	SKD -61	0.58	6.237	6.05	-	Training
7	SKD -62	2.19	5.66	5.8	Inactive	Training
8	SKD -63	0.44	6.357	6.26	-	Training
9	SKD -67	0.35	6.495	6.56	-	Training
10	SKD -71	0.22	6.658	6.52	-	Training
11	SKD -72	0.34	6.469	6.44	-	Training
12	SKD -73	0.29	6.538	6.63	-	Training
13	SKD -74	0.4	6.398	6.08	-	Test
14	SKD -75	1.32	5.879	6.02	-	Training
15	SKD -76	0.68	6.167	6.14	-	Training
16	SKD -77	0.11	6.959	7.11	-	Training
17	SKD-78	0.36	6.444	6.48	-	Test
18	SKD -79	0.17	6.77	6.89	-	Training
19	SKD -80	0.095	7.022	6.83	-	Test
20	SKD -81	0.11	6.959	6.26	-	Test
21	SKD-82	0.12	6.921	6.77	-	Training
22	SKD -83	0.077	7.114	7.07	-	Training
23	SKD -84	0.12	6.921	6.91	-	Training
24	SKD -85	0.085	7.071	7.14	-	Training
25	SKD -86	0.12	6.921	6.73	-	Training
26	SKD -87	0.077	7.114	6.95	-	Test
27	SKD -88	1.16	5.936	5.94	-	Training
28	SKD -89	1.55	5.81	5.88	-	Training
29	SKD -90	0.13	6.886	6.89	-	Training
30	SKD -91	0.41	6.387	6.49	-	Training
31	SKD -92	0.41	6.229	6.38	-	Test
32	SKD -96	0.97	6.013	6.27	-	Training
33	SKD -97	0.51	6.292	6.66	-	Training

34	SKD -98	1.07	5.971	6.03	-	Training
35	SKD -99	0.45	6.347	6.15	-	Training
36	SKD-100	0.52	6.284	6.27	-	Training
37	SKD -103	0.058	7.237	7.35	-	Training
38	SKD -104	0.025	7.602	7.56	Active	Training
39	SKD -105	0.053	7.276	7.25	-	Training
40	SKD -106	0.052	7.284	7.23	-	Training
41	SKD -107	0.29	6.538	6.45	-	Training
42	SKD-108	0.044	7.357	6.92	-	Test
43	SKD -109	0.18	6.745	6.66	-	Training
44	SKD -110	0.054	7.268	7.25	-	Training
45	SKD-111	0.36	6.444	6.5	-	Training
46	SKD -112	0.1	4.996	5.51	Inactive	Training
47	SKD -113	0.1	7	6.83	-	Training
48	SKD -114	0.08	7.097	7.05	-	Training
49	SKD -115	0.052	7.284	7.07	-	Test
50	SKD -116	0.071	7.149	7.19	-	Training
51	SKD -117	0.1	7	7.34	-	Test
52	SKD -118	0.029	7.538	7.36	Active	Training
53	SKD -119	0.028	7.553	7.37	Active	Training
54	SKD-120	0.047	7.328	7.24	-	Training
55	SKD -121	0.025	7.602	7.25	Active	Test
56	SKD -122	0.025	7.602	7.43	Active	Test
57	SKD -123	0.17	6.77	6.68	-	Test
58	SKD -124	0.056	7.252	7.31	-	training
59	SKD -125	0.038	7.42	7.41	-	Training
60	SKD -126	0.043	7.367	7.42	-	Training
61	SKD -127	0.23	6.638	6.78	-	Test
62	SKD -128	0.13	6.886	6.36	-	Test
63	SKD -129	0.054	7.268	7.24	-	Test
64	SKD -130	0.052	7.284	7.23	-	Test
65	SKD-131	0.023	7.638	7.57	Active	Training
66	SKD -132	0.074	7.131	7.21	-	Test
67	SKD -133	0.055	7.26	7.24	-	Training
68	SKD -134	0.17	6.77	6.73	-	Training
69	SKD -136	0.082	7.086	7.15	-	Training
70	SKD -137	0.14	6.854	6.9	-	Training
71	SKD -138	0.92	6.036	6.58	-	Test
72	SKD -139	0.46	6.337	6.74	-	Test
73	SKD -140	0.16	6.796	6.78	-	Training
74	SKD -143	1.19	5.924	6.15	-	Training
75	SKD -145	0.23	6.638	6.5	-	Training
76	SKD -146	1.4	5.854	5.79	-	Training
77	SKD -147	1.15	5.939	5.76	-	Training
78	SKD -148	0.54	6.268	6.33	-	Training
79	SKD -149	0.51	6.292	0.16	-	Test
80	SKD -151	0.8	6.097	6.07	-	Training
81	SKD -152	1.3	5.886	6.29	-	Test
82	SKD -153	0.9	6.046	5.79	-	Training
83	SKD -156	1.6	5.796	6.5	Inactive	Test
84	SKD -157	0.65	6.187	6.25	-	Training
85	SKD -158	0.47	6.328	6.24	-	Training
86	SKD -159	0.13	6.886	7.01	-	Training
87	SKD -160	1.3	5.886	6.09	-	Test
88	SKD -162	1.1	5.959	6.07	-	Training
89	SKD -163	0.48	6.319	6.31	-	Training
90	SKD -164	0.33	6.481	6.39	-	Training
91	SKD -165	0.38	6.42	6.41	-	Training
92	SKD -166	1.4	5.854	6.08	-	Test

93	SKD -167	0.37	6.432	6.43	-	Training
94	SKD -168	1.2	5.921	5.77	-	Training
95	SKD -169	0.32	6.495	6.56	-	Training
96	SKD -170	0.7	6.155	5.9	-	Test
97	SKD -171	1.1	5.959	5.97	-	Test
98	SKD -172	1.3	5.886	5.8	-	Training
99	SKD -174	0.075	7.125	7.21	-	Training
100	SKD -175	0.106	6.975	7.1	-	Training
101	SKD -176	0.039	7.409	7.15	-	Test
102	SKD -177	0.026	7.585	7.04	Active	Test
103	SKD -178	0.034	7.469	7.52	-	Training
104	SKD -179	0.029	7.538	7.08	Active	Test
105	SKD -180	0.028	7.553	7.25	Active	Test
106	SKD -181	0.028	7.553	7.1	Active	Test
107	SKD -182	0.024	7.62	7.28	Active	Test
108	SKD -183	0.03	7.523	7.53	Active	Training
109	SKD -184	0.032	7.495	6.87	-	Test
110	SKD-185	0.04	7.398	7.4	-	Training
111	SKD -186	0.354	6.451	6.52	-	Training
112	SKD -187	1.16	5.936	5.79	-	Training
113	SKD -188	0.178	6.75	6.73	-	Training

Alignment of molecules

For 3D QSAR study all the molecules in data set must have relative conformation that can be aligned over their common scaffold. All the molecules in the data set bear a common basic scaffold i.e biphenyl benzofuran & benzothiophene (figure-1). Alignment can be done using pharmacophore based molecular alignment protocols for the present study.

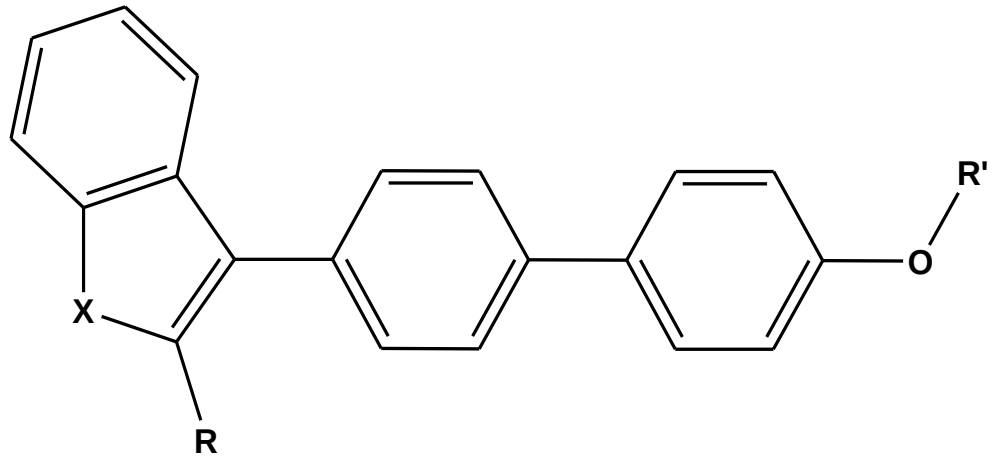

X= O or S

Figure 1. Basic skeleton Benzofuran and Benzothiophene Biphenyls as PTP 1B inhibitor

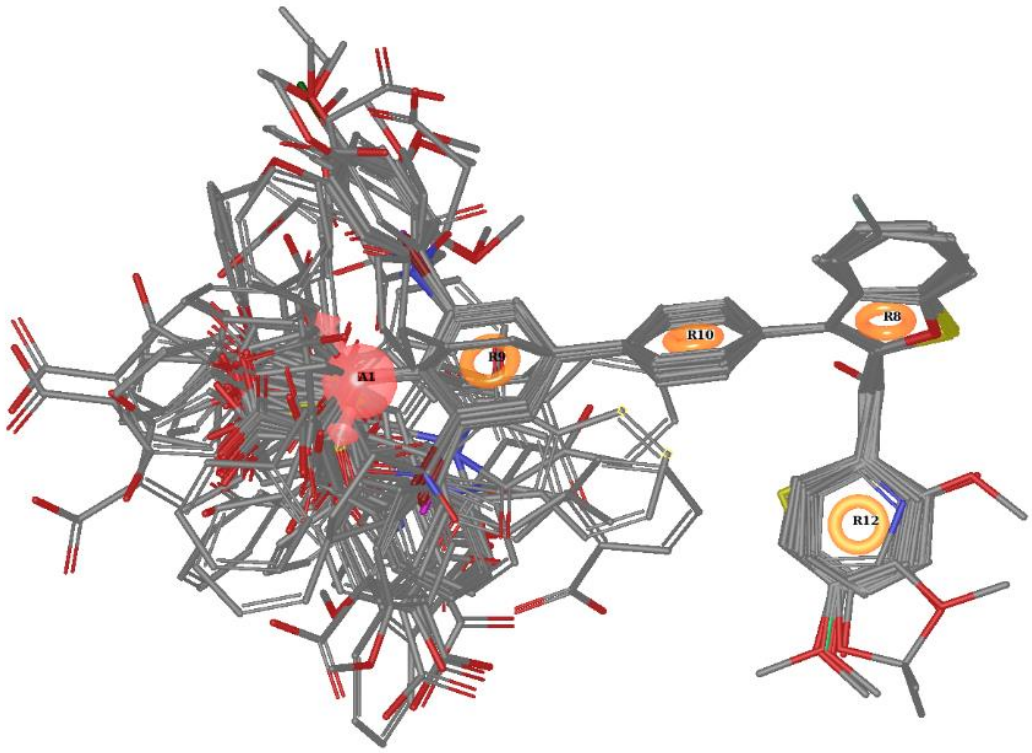

Fig. 2 Alignment of the all Molecules with common Pharmacophore

Molecular modeling and computational details

The study was performed using the PHASE software that is a versatile product for pharmacophore perception, structural alignment, activity prediction and 3D database creation and searching. Three dimensional structures of all molecules were sketched using freely available Discovery Studio visulizer version 2.1. After the sketching of all molecules, cleaning and conformational search was performed in "develop pharmacophore" module of PHASE. Conformers for all molecules were generated employing following specification i.e mixed MCMM/LMOD method, OPLS_2005 force field, 5 conformers per rotatable bond and maximum of 1000 conformers with relative energy difference of 10 kcal/mol. The conformers were further treated with GB/SA water and 100 minimization steps. The criterion for removal of redundant conformers was set to RMSD of 1Å. Finally these conformers were employed for the development of pharmacophore model and 3D QSAR studies.

Pharmacophore and 3D QSAR modeling

The generated conformations of all molecules were employed for the development of the pharmacophore model. The model is developed on the basis of active molecules. The generated models are ranked on the basis of scoring protocol i.e. scoring parameters like survival, survival minus inactives (S-I) and post-hoc. Survival score corresponds to score actives, S-I to score inactives and post-hoc to rescore. High values of score actives are calculated for the pharmacophore hypotheses that are according to the active ligands only whereas survival-inactives are for the hypotheses that have good power to discriminate the active ligands from the inactive ones. The best selected hypothesis on the basis on above criteria was then used for the alignment of all study molecules. For the development of QSAR model all molecules with their pharmacophoric features aligning over the generated hypothesis were placed into regular grid of cubes (1Å) with each cubes allotted 0 or 1 'bits' to account for the different type of pharmacophoric features in the training set that occupy the cube (1Å). This representation gives rise to huge pool of binary values that can be used as independent variables to create 3D QSAR models. This large number of independent variables is then correlated with dependent variables using Partial least squares (PLS) analysis.[29]

PLS analysis and model validation

PLS analysis is an extension to the multiple regression analysis and is used to correlate the large number of independent variables with dependent variable for the development of QSAR model. PHASE QSAR models were generated using maximum of N/5 PLS factors, where N corresponds to number of molecules in the training set. To improve the signal to noise ratio 't-value' less than 2 were employed prior to run PLS

analysis. The best model is selected on the basis of highest values of R^2 (correlation of prediction for the training set), SD (standard deviation) and F-value. The model was validated by determining Q^2 (cross validation correlation for the test set molecules), Pearson-r (to check the external predictability of model) and k, k′, R^2_o, R'^2_o.

Pharmacophore modeling and its validation

After performing the sketching, cleaning and conformers generation the data set was divided into actives, inactives and moderately actives for the generation of pharmacophore model. Molecules with pIC50 higher than 7.523 and lower than 5.796 were considered to be actives and inactives respectively, whereas those in between these limits were considered to be moderately active [Table I]. Sites were then created for all molecules that give total six kinds of markers i.e acceptor, donor, hydrophobic, positive ionization, negative ionization and ring aromatic features. For the generation of pharmacophore model numbers of minimum and maximum sites were selected as five. Furthermore, the software was restricted to match five out of six selected active ligands. Finally, common pharmacophore models were scored and top ten hypotheses were survived to the PHASE scoring procedure i.e survival. Results of score hypothesis are shown in Table II. The best hypothesis ARRRR 389 were selected on the basis of highest values of survival and vector. The stereo view of ARRRR 389 and its mapping with the highest active molecule SKD-131 having fit value of 3 is displayed in Figure 5 and 6 respectively. Further, selected best pharmacophore model needed to be validated for its power to identify actives and inactives.

Table II. Scoring results of the generated various pharmacophore hypotheses

Sr. No	Hypothesis ID	Survival	Site	Vector	Volume	# Matches
1	ARRRR. 389	61.963	0.93	0.976	0.718	12
2	ARRRR. 378	61.915	0.91	0.973	0.688	12
3	ARRRR. 381	61.910	0.92	0.960	0.688	12
4	ARRRR. 376	61.878	0.96	0.977	0.742	12
5	ARRRR. 525	61.872	0.88	0.959	0.693	12
6	ARRRR. 469	61.751	0.91	0.962	0.677	12

Generation of 3D QSAR Model and its validation

3D QSAR is a well known technique to correlate 3D structure features with the biological activity of the molecules. The pharmacophore based alignment bundle of 113 molecules was used to develop 3D QSAR model. PHASE has two modules for performing 3D QSAR i.e atom based and pharmacophore based. The difference among both is whether all atoms are taken into account, or merely the pharmacophore sites that can be matched to the hypothesis. Pharmacophore based QSAR works well for the molecules having structural diversity or having high number of rotatable bonds. For present study of congenric dataset molecules, atom based 3D QSAR is best suited. Basically, in this QSAR study the activity data of the study molecules is correlated with relative 3D positions of the atoms present in ligands.

To build QSAR model, the dataset was randomly divided into training and test set of 80 and 33 compounds respectively, in order to create training set to test set ratio of 3:1.Grid spacing of 1Å and the maximum PLS factors as 5 were employed to develop the model. The statistically best model corresponding to PLS 5 ($ARRRR.389_5$) was selected on the basis of highest values of R^2, 0.9527; SD, 0.1276; and F-value, 297.8. The results of all models corresponding to number of PLS factors are displayed in Table III. The correlation graph between experimental and predicted activities of training set molecules from the best model is displayed in Figure 3. The best model was validated for its stability (Q^2) and reliability to predict the biological activity of the molecules that have not been used for the development of model i.e. test set molecules (Pearson-r). The model showed good values of Q^2 and pearson-r i.e. 0.3655 and 0.611 respectively. The correlation graph between experimental and predicted activities of test set molecules is displayed in Figure 4. Only the high values of R^2 and Q^2 is not the sufficient criteria for the validation of generated QSAR models however the model should satisfy $q^2 > 0.5$, $R^2 > 0.6$, R^2_o or R'^2_o close to R^2, and the corresponding $0.85 \leq k \leq 1.15$ or $0.85 \leq k' \leq 1.15$. The best model showed satisfactory values of k, 0.998; k', 1.001; R^2_o, 0.999 and R'^2_o, 0.999. These all parameters further strengthen the stability and reliability of generated QSAR model.

Table III. Statistic results of generated 3D QSAR models employing ARRRR. 389 based alignment.

Model ID	#PLS Factors	SD	R^2	F	Stability	RMSE	Q^2	Pearson-r

ARRRR.389$_1$	**1**	**0.3402**	**0.6452**	**141.9**	**0.9747**	**0.5363**	**0.5363**	**0.7711**
ARRRR. 389$_2$	**2**	**0.2321**	**0.8371**	**197.8**	**0.9009**	**0.4252**	**0.5323**	**0.7385**
ARRRR. 389$_3$	**3**	**0.1877**	**0.8948**	**215.5**	**0.856**	**0.4555**	**0.4634**	**0.6865**
ARRRR. 389$_4$	**4**	**0.1646**	**0.9202**	**216.2**	**0.8393**	**0.4656**	**0.4393**	**0.6687**
ARRRR. 389$_5$	**5**	**0.1276**	**0.9527**	**297.8**	**0.7874**	**0.4953**	**0.3655**	**0.611**

Model ID *(ARRRR.389$_x$) corresponds to QSAR model with PLS factor x employing ARRRR.389 based alignment.*
SD : Standard deviation
R^2 : correlation of prediction for training set molecules
F-value : Fisher test
RMSE : Root means squared error
Q^2 : Cross validation correlation for test set molecules
Pearson-r :Correlation coefficient for test set molecules

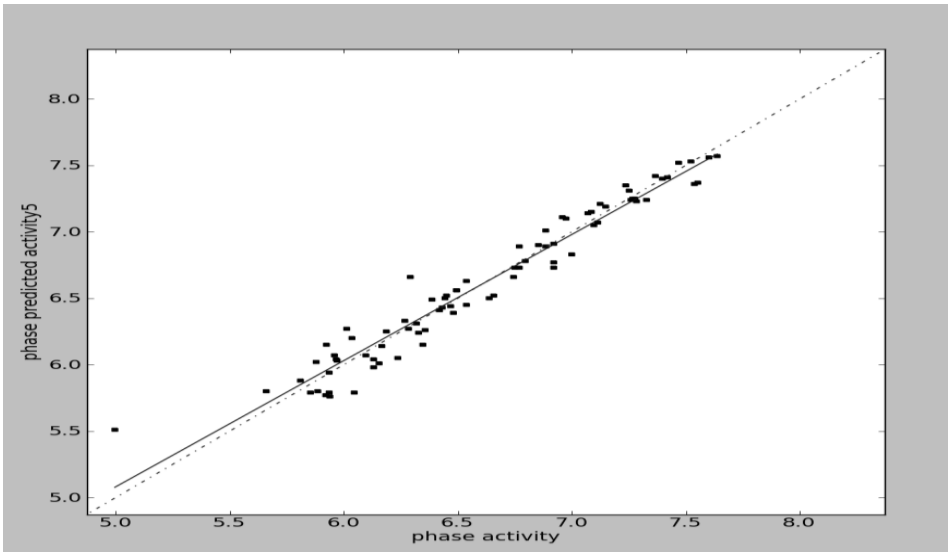

Figure 3 Co-relationship between Phase activity (Actual PIC_{50} Value) Vs Phase predicted (Predicted PIC_{50} Value) for the molecules of training set

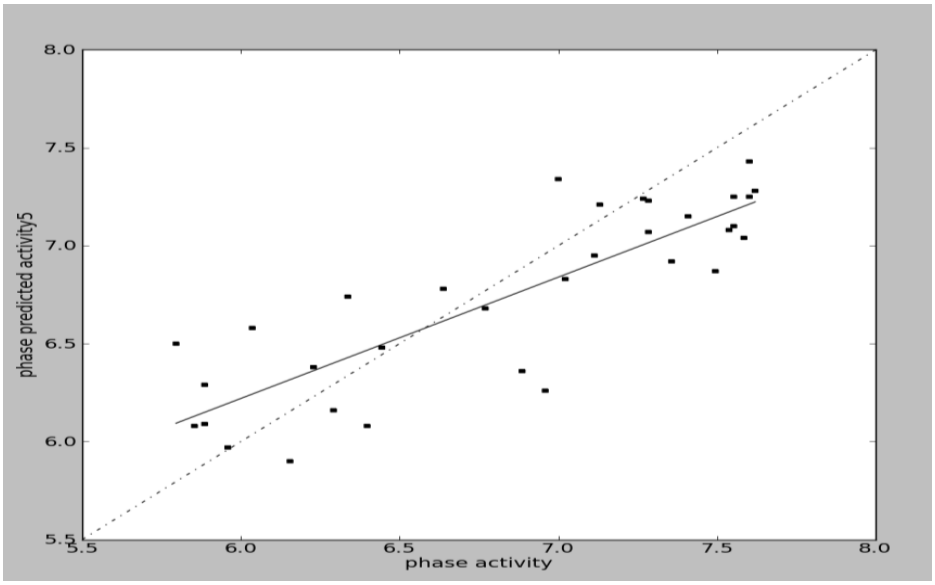

Figure 4 Co-relationship between Phase activity (Actual PIC_{50} Value) Vs Phase predicted (Predicted PIC_{50} Value) for the molecules of test set

3D contours analysis

During the alignment of molecules, all molecules align with their least energy conformers over the pharmacophore features of the generated hypothesis. It suggests that not only the substitution but the orientation changes of molecules caused by the substitutions (lower energy conformer of molecule among the total number of generated conformations tries to fit itself over the pharmacophore sites) also have an impetus on the biological activity. 3D contours of different properties are analyzed one by one to explain structural features governing biological activities of molecules present in data sets.

Negative Ionizable property contours

Negative Ionizable (NI) property contour map is shown in Figure 5, In this figure the red colored cubes represent the areas where the presence of NI group is unfavorable and may lead to decrease in the biological activity whereas blue colored cubes indicates the NI favorable regions Ionization of -COOH group will affect the biological activity, if it is negatively ionized it will increase the activity like in molecule SKD 131 in which –COOH group is negatively ionized as compared to molecule SKD 112 in which –COOH group is in unionized form . Finally if we will substitute the negatively ionized -COOH group by highly negatively ionized group or improve the negative ionization at that position, activity of the molecules will be improved. In molecule SKD 104, 121, 122, the –COOH group is negatively ionized but to a lesser extent as compared with molecule SKD 131, hence they will exhibit activity which is slightly less than that of SKD 131. Similarly molecule SKD 125 and 130 has less activity than SKD 131 due to less negatively ionized –COOH group. In molecule 109, 123 and 128 the negative ionization of –COOH group Is decreasing which will decrease the activity of these molecules. In molecule SKD 100, removal of –COOH group cause marked reduction in activity. In molecule SKD 75 and 187 no ionization of –COOH seems to occur thus decreasing the activity to several times as compared with that of SKD 131.

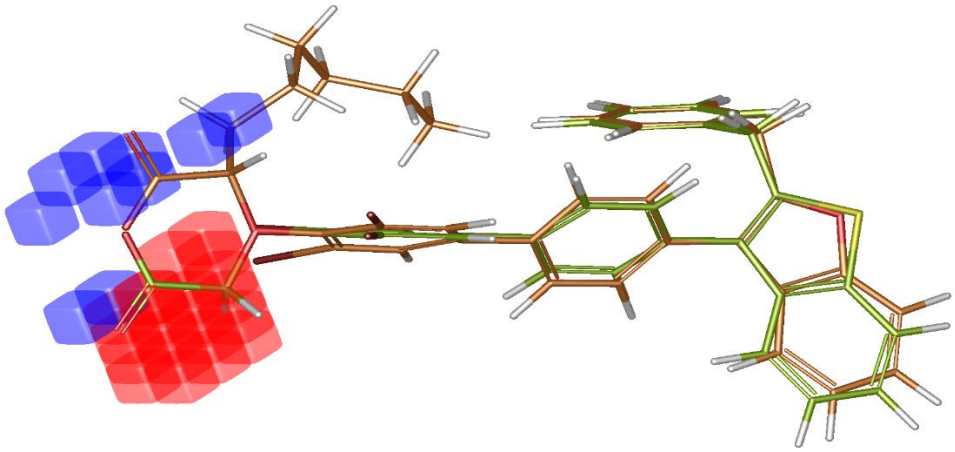

Figure 5. Contour map of negative ionizable property with the highest active molecule (SKD-131) and inactive molecule (SKD-112)

Electron withdrawing property contours

Electron withdrawing (EW) property contour map is shown in Figure 6. Red coloured contour correspond to the areas where the presence of EW groups may lead to suppression of activity, whereas blue coloured corresponds to areas where electron withdrawing groups may enhance the biological activity of the molecules. Electron withdrawing group present near to biphenyl ring will decrease the activity of the compound (unfavorable site). In molecule SKD 112, electron withdrawing group is near to biphenyl ring and activity decreases as compared to molecule SKD 131 in which electron withdrawing group is far from biphenyl ring. If Br which is attached to the biphenyl ring is replaced by p/m-OCH_3 benzene or iodine or is removed as in case of molecule SKD 121, 122, 100, 75, 177, it will decrease the activity as compared with activity of SKD 131. If the alkyl chain attached adjacent to –COOH group is replaced by benzene or its length is shortened as in case of molecule SKD 125, 128, 130, it will decrease the activity as compared with activity of SKD 131.

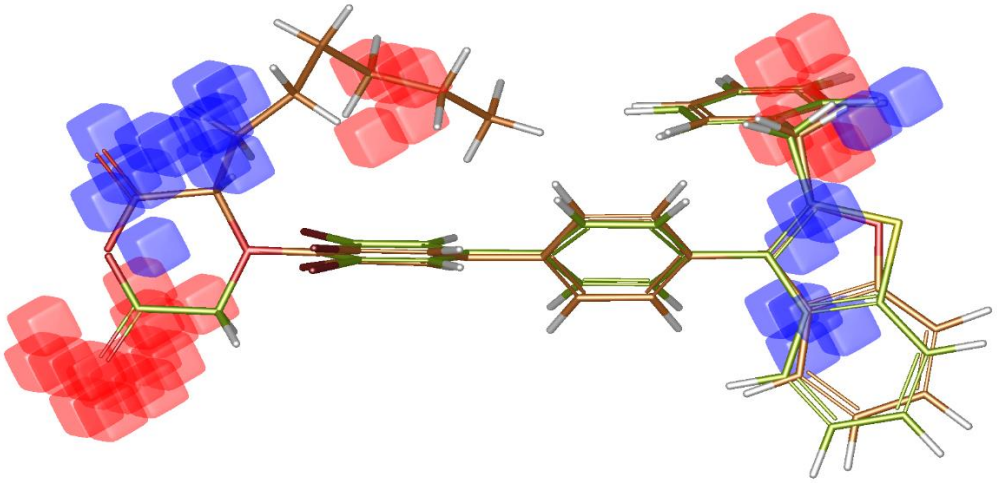

Figure 6. Contour map of electron withdrawing property with the active molecule (SKD-131) and Inactive molecule (SKD-112)

Hydrophobic property contour

Hydrophobic property contour map is shown in Figure 7 in this figure Hydrophobicity also play major role in this series of molecules and affect the activity of the molecules. Hydrophobicity at the near of biphenyl ring will decrease the activity or hydrophobicity around the biphenyl ring will decrease the activity (unfavorable site). Molecule SKD 112 having a hydrophobic group close to the biphenyl ring which will decrease the activity. Thus if the hydrophobicity or hydrophobic group is near from biphenyl ring, they will decrease the activity like in molecule SKD 75, 100, 112, 157,187 in which the distance of hydrophobic group is less as compared to molecules SKD 131, 121 and 104 and activity will increase.

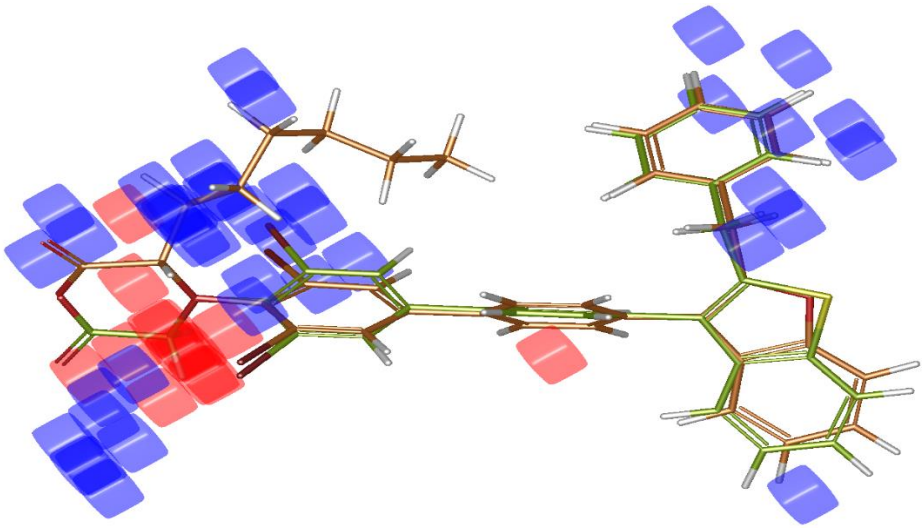

Figure 7. Contour map of hydrophobic property with the highest active molecule (SKD-131) and inactive molecule (SKD-112)

Database screening (in-house database)

The best pharmacophore model ARRRR.389_5 was used as a three dimensional query for screening of an in-house database of about 15,00,000 compounds. During the screening software was relaxed to match database molecules with at least 3 sites of pharmacophore hypothesis. In the screening total 20 molecules were retrieved having different parent scaffolds. Among these molecules 12 molecules were having the parent scaffold similarity with the study molecules. Among these molecules, six best molecules on the basis of their high fitness value are displayed in Table IV along with their mapping over hypothesis ARRRR.389_5.

Results and discussion

The present study is a combination of pharmacophore modeling and 3D QSAR analysis. Both studies have been performed using PHASE 2.5 embedded into Maestro 9.1 running on centOS

5.4 operating system installed in hp Z200 workstation. The generated pharmacophore model is employed for the alignment of all study molecules with their pharmacophoric sites and for the screening of in-house database to find out new molecules that may have PTP 1B inhibitory activity. The QSAR model generated from the dataset is employed to reveal the important information about the substitution pattern of molecules and relationship with their corresponding biological activity. QSAR model was also used to predict the biological activity of the molecules retrieved from the screening of database. There are several steps that are carried out for the development of pharmacophore and 3D QSAR model i.e. prepare ligands, cleaning structures, conformer generation, create sites, find common pharmacophore, score hypothesis and finally the build QSAR model.

Conclusion

On the basis of above study it can be concluded that the developed pharmacophore can be used as a tool for the alignment of all the study molecules for generation of the highly predictive QSAR. Generated QSAR model is further used for the prediction of the biological activity of new compounds. The contour analysis of the best QSAR model clearly indicates that hydrophobic property is the most important determinant for inhibition of PTP 1B than the electron withdrawing and hydrogen bond donor properties. Virtual screening (VS) of in house database of approximately sixty thousand molecules using best model retrieve twelve new PTP 1B inhibitors. Thus, this study guided how to design new potent PTP 1B inhibitors as novel agents for the management of diabetes.

Acknowledgement:

The authors are thankful to the **Department of Pharmaceutical Sciences and Drug Research, Punjabi University**, Patiala, Punjab, India, for providing us the computational facility and resources for completing the research work.

References:

1. Alonso, A. et al. (2004) Protein tyrosine phosphatases in the human genome. Cell117, 699–711.
2. Zhang, Z.Y. (2001) Protein tyrosine phosphatases: prospects for therapeutics. Curr. Opin. Chem. Biol. 5, 416–423
3. Andersen, J.N. et al. (2004) A genomic perspective on protein tyrosine phosphatases: gene structure, pseudogenes, and genetic disease linkage. FASEB J. 18, 8–30
4. Arena, S. et al. (2005) Genetic analysis of the kinome and phosphatome in cancer.Cell. Mol. Life Sci. 62, 2092–2099
5. van Huijsduijnen, R.H. et al. (2002) Selecting protein tyrosine phosphatases as drug targets. Drug Discov. Today 7, 1013–1019
6. Bialy, L. and Waldmann, H. (2005) Inhibitors of protein tyrosine phosphatases: next-generation drugs? Angew. Chem. Int. Ed. Engl. 44, 3814–3839
7. Zhang, Z.-Y. and Lee, S.-Y. (2003) PTP1B inhibitors as potential therapeutics in the treatment of type 2 diabetes and obesity. Expert Opin. Investig. Drugs 12,223–233
8. Tonks, N.K. (2003) PTP1B: from the sidelines to the front lines! FEBS Lett. 546, 140–148
9. Bandyopadhyay, D. et al. (1997) Protein-tyrosine phosphatase 1B complexes with the insulin receptor in vivo and is tyrosine-phosphorylated in the presence of insulin.J. Biol. Chem. 272, 1639–1645
10. Dadke, S. et al. (2000) Down-regulation of insulin signalling by protein-tyrosine phosphatase 1B is mediated by an N-terminal binding region. J. Biol. Chem. 275, 23642–23647
11. Walchli, S. et al. (2000) Identification of tyrosine phosphatases that dephosphorylate the insulin receptor: a brute-force approach based on 'substratetrapping' mutants. J. Biol. Chem. 275, 9792–9796
12. Goldstein, B.J. et al. (2000) Tyrosine dephosphorylation and deactivation of insulin receptor substrate-1 by protein-tyrosine phosphatase 1B. Possible facilitation by the formation of a ternary complex with the Grb2 adaptor protein. J. Biol. Chem. 275,4283–4289
13. Calera, M.R. et al. (2000) Dynamics of protein-tyrosine phosphatases in rat adipocytes. J. Biol. Chem. 275, 6308–6312
14. Ahmad, F. et al. (1995) Osmotic loading of neutralizing antibodies demonstrates a role for protein-tyrosine phosphatase 1B in negative regulation of the insulin action pathway. J. Biol. Chem. 270, 20503–20508
15. Kenner, K.A. et al. (1996) Protein-tyrosine phosphatase 1B is a negative regulator of insulin- and insulin-like growth factor-I-stimulated signalling. J. Biol. Chem. 271,19810–19816
16. Byon, J.C.H. et al. (1998) Protein-tyrosine phosphatase-1B acts as a negative regulator of

insulin signal transduction. Mol. Cell. Biochem. 182, 101–198
17. Zinker, B.A. et al. (2002) PTP1B antisense oligonucleotide lowers PTP1B protein, normalizes blood glucose, and improves insulin sensitivity in diabetic mice. Proc. Natl. Acad. Sci. U. S. A. 99, 11357–11362
18. Di Paola, R. et al. (2002) A variation in 3‘UTR of hPTP1B increases specific gene expression and associates with insulin resistance. Am. J. Hum. Genet. 70, 806–812
19. Echwald, S.M. et al. (2002) A P387L variant in protein tyrosine phosphatase-1B (PTP-1B) is associated with type 2 diabetes and impaired serine phosphorylation of PTP- 1B in vitro. Diabetes 51, 1–6
20. Mok, A. et al. (2002) A single nucleotide polymorphism in protein tyrosine phosphatase PTP-1B is associated with protection from diabetes or impaired glucose tolerance in Oji-Cree. J. Clin. Endocrinol. Metab. 87, 724–727
21. Elchebly, M. et al. (1999) Increased insulin sensitivity and obesity resistance in mice lacking the protein tyrosine phosphatase-1B gene. Science 283, 1544–1548
22. Klaman, L.D. et al. (2000) Increased energy expenditure, decreased adiposity, and tissue-specific insulin sensitivity in protein-tyrosine phosphatase 1B-deficient mice.Mol. Cell. Biol. 20, 5479–5489
23. Zabolotny, J.M. et al. (2002) PTP1B regulates leptin signal transduction in vivo. Dev.Cell 2, 489–495
24. Zhang, Z.Y. (2002) Protein tyrosine phosphatases: structure and function, substrate specificity, and inhibitor develo-pment. Annu. Rev. Pharmacol. Toxicol. 42, 209–234
25. Shen, K. et al. (2001) Acquisition of a specific and potent PTP1B inhibitor from a novel combinatorial library and screening procedure. J. Biol. Chem. 276, 47311–47319
26. Phase, Version 2.5, User Manual, Schrodinger Press, LLC, New York, 2005.
27. Malasmas, M.S. et al. (2000) Novel benzofuran and benzothiophene biphenyls as inhibitors of protein tyrosine phosphatase 1B with antihyperglycemic properties. J. Med. Chem. 43,1293-1310.
28. Lanzetta, P.A. et al. (1979) An improved assay for nanomolar amounts of inorganic phosphate. Anal. Biochem. 100, 95-97.
29. Dixon, S.L. et al. (2006) Phase : A new engine for pharmacophopre perception, 3D QSAR model development and 3D database screening: Methodology and prelimenary results. J. Comput. Aided Mol. Des. 20, 647-671.